Sentinel-1 SAR Backscatter Response to Agricultural Drought in The Netherlands

Shorachi, Maurice ; Kumar, V.; Steele-Dunne, S.C.

DOI
10.3390/rs14102435

Publication date
2022

Document Version
Final published version

Published in
Remote Sensing

remote sensing

MDPI

Article

Sentinel-1 SAR Backscatter Response to Agricultural Drought in The Netherlands

Maurice Shorachi [1], Vineet Kumar [2,*] and Susan C. Steele-Dunne [2]

[1] Department of Water Management, Delft University of Technology, Stevinweg 1, 2628 CN Delft, The Netherlands; mshorachi@gmail.com
[2] Department of Geoscience and Remote Sensing, Delft University of Technology, Stevinweg 1, 2628 CN Delft, The Netherlands; s.c.steele-dunne@tudelft.nl
* Correspondence: v.kumar-1@tudelft.nl

Abstract: Drought is a major natural hazard that impacts agriculture, the environment, and socio-economic conditions. In 2018 and 2019, Europe experienced a severe drought due to below average precipitation and high temperatures. Drought stress affects the moisture content and structure of agricultural crops and can result in lower yields. Synthetic Aperture Radar (SAR) observations are sensitive to the dielectric and geometric characteristics of crops and underlying soils. This study uses data from ESA's Sentinel-1 SAR satellite to investigate the influence of drought stress on major arable crops of the Netherlands, its regional variability and the impact of water management decisions on crop development. Sentinel-1 VV, VH and VH/VV backscatter data are used to quantify the variability in the spatio-temporal dynamics of agricultural crop parcels in response to drought. Results show that VV and VH backscatter values are 1 to 2 dB lower for crop parcels during the 2018 drought compared to values in 2017. In addition, the growth season indicated by the cross-ratio (CR, VH/VV) for maize and onion is shorter during the drought year. Differences due to irrigation restrictions are observed in backscatter response from maize parcels. Lower CR values in 2019 indicate the impact of drought on the start of the growing season. Results demonstrate that Sentinel-1 can detect changes in the seasonal cycle of arable crops in response to agricultural drought.

Keywords: agriculture; crops; cross-ratio; drought; Sentinel-1; Synthetic Aperture Radar; irrigation

Citation: Shorachi, M.; Kumar, V.; Steele-Dunne, S.C. Sentinel-1 SAR Backscatter Response to Agricultural Drought in The Netherlands. *Remote Sens.* **2022**, *14*, 2435. https://doi.org/10.3390/rs14102435

Academic Editors: Luca Brocca, Massimiliano Pasqui and Ramona Magno

Received: 11 April 2022
Accepted: 17 May 2022
Published: 19 May 2022

1. Introduction

The threat to global food security is expected to increase as a result of climate change and the rising world population [1,2]. Monitoring agricultural crops to predict yield, predict change in water use efficiency and detect the impact of extreme weather events is vital for ensuring long-term food security. Drought is an abiotic stress that arises from a soil moisture deficit when the availability of precipitation does not meet evaporative demand, and can lead to a reduction in crop yields [3–5]. A reduction in crop yield can be caused by the shorter life-cycle of the crops, and/or the adaptation of the stomatal control and reduction of leaf area in order to cope with drought stress [6]. Future climate change is expected to increase the frequency of severe meteorological [7–9] and agricultural droughts [4,10]. Large-scale, continuous monitoring is essential to detect, monitor and mitigate the effects of drought on agricultural production.

Drought indices from meteorological station-based weather information are effective for drought assessment [11–13]. However, the global distribution of meteorological stations is highly variable in space and time, limiting their potential use for drought monitoring [14–16]. Remote sensing satellite observations provide continuous, global coverage and can provide insight into droughts at a range of resolutions [17–19]. Many studies have used spectral indices from the visible to near infra-red part of the spectrum (e.g., [20–24]). However, their reliability is limited by cloud cover. Microwave remote sensing offers continuous coverage without being hindered by atmospheric conditions.

Synthetic Aperture Radar (SAR) data have been widely used in vegetation monitoring studies due to microwave sensitivity to dielectric and geometric changes during crop development [25,26]. However, the use of several previous and existing SAR missions viz. RADARSAT-1/2, ALOS-1/2 and TerraSAR-X was limited due to spatial coverage and coarse temporal resolution. With the launch of the Sentinel-1 SAR constellation [27], it is possible to have 12 days (6 days in Europe) of temporal resolution data across the globe and high temporal resolution over the Europe (<2 days depending on the latitude) by combining different acquisitions in interferometric wide (IW) swath mode. Additionally, Sentinel-1 SAR archive and real-time data accessibility in cloud computing servers, such as Google Earth Engine (GEE), allows for large scale monitoring without the constraints of data handling and processing [28].

The potential of Sentinel-1 SAR data have been shown in many studies for crop growth monitoring [29–31], phenology tracking [32] and biophysical parameter estimation [33]. The high temporal resolution, the fact that acquisitions are unaffected by cloud cover, and the sensitivity of backscatter to vegetation water content and geometry means that Sentinel-1 offers unique potential to capture the drought response of crops. However, limited research has been conducted to understand the potential of Sentinel-1 SAR signal response to the agricultural drought events [34,35].

Two consecutive drought summers occurred across central Europe in 2018 and 2019 [36–39]. Hari et al. [9] found that the consecutive droughts of 2018–2019 were the most severe in the last 250 years. These droughts had a severe impact in the Netherlands [40–42], resulting in a significant drop in yield for most crops [43]. The long term average precipitation during the summer growing season (April to September) is 438 mm. However, in 2018 this was just 304 mm [40]. The drought in 2018 caused a peak in agricultural water usage in the Netherlands and a lowering of the groundwater table, particularly in the southeast [42]. Water deficit influences crop water content and structure. Droughts have an adverse effect on the overall yield, which is caused by a reduction in leaf area, adaptation of the stomatal control and the shorter life-cycle of the crops to cope with the water deficit [6]. Since the SAR response depends on the geometrical and dielectric properties, it is expected that the water deficit caused by the drought will be observable in the SAR response.

Here, we compare the seasonal cycle of Sentinel-1 SAR observables across the Netherlands from several crops during drought-affected years to those of a normal year. Differences in the Sentinel-1 observables will be discussed with respect to rainfall, soil moisture and regional crop yield estimates during the drought-affected and normal years. We also examine the influence of Sentinel-1 viewing geometry and acquisition time. We investigate whether spatial variability in the drought response due to crop and soil type, irrigation water availability can be detected in the SAR observalbes (VV, VH backscatter and VH/VV ratio).

2. Data and Methods

2.1. Study Area

This study is focused on the impact of the 2018 and 2019 droughts in the Netherlands. The study areas, shown in Figure 1, were selected to account for different soil types, irrigation practices and the spatial distribution of drought in the Netherlands during 2018 and 2019, as well as the availability of in situ information. The general study area comprises three areas indicated in blue. Three factors were considered in the definition of the areas of interest. First, the yield data are available at province level. Second, water management decisions are made by water boards. These are regional governing bodies responsible for the management of surface water in the environment. Their boundaries do not coincide with province boundaries. Third, we need to consider the location of areas of interest within the swaths of the Sentinel-1 relative orbits. In Figure 1, the Vechstromen-Noord area consists of the northern part of the Vechstromen water board, which includes parts of the Drenthe and Overijssel provinces. Vechtstromen-Noord is observed in Sentinel-1 relative orbits (ROs) 37, 139, 88 and 15. Scheldestromen consists of the part of the Scheldestromen water board that falls within the Zeeland province. Common crop parcels within RO 37,

110, 88 and 161 swaths were selected from Scheldestromen. Finally, the Flevopolder is an island of reclaimed land, and is part of the Zuiderzeeland water board. It is an area characterized by highly productive, intensive agriculture and has featured in many SAR studies [29,44,45].

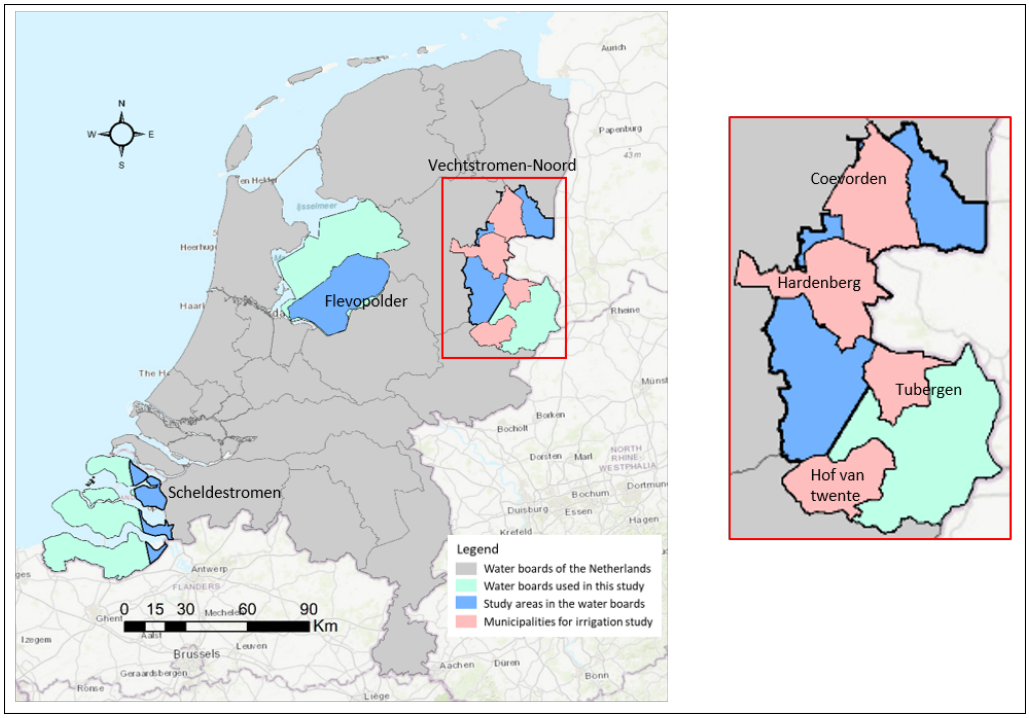

Figure 1. The location of three areas of interest (blue) in province map of the Netherlands. Vechtstromen-Noord, Flevopolder and Scheldestromen areas are part of the Vechtstromen, Zuiderzeeland and Scheldestromen water boards. The inset shows the municipalities within the Vechtstromen water board used to study the effect of irrigation practices.

The difference in soil texture and water management among the areas is expected to lead to a variation in drought response. The clay content of soil in Flevopolder is relatively high. In contrast, the soil in Vechtstromen-Noord has a high sand content. Crops in Zeeland (including the Scheldestromen area) suffered yield loss due the lack of precipitation and the ban on the open water irrigation.

To investigate the potential influence of water management (e.g., irrigation availability), we compared data from four municipalities of the Vechtstromen waterboard, highlighted in red in the inset of Figure 1. In Coevorden and Hardenberg, irrigation is only available from groundwater during droughts. In contrast, farmers in Tubbergen and Hof van Twente have access to both surface (open) water and groundwater for irrigation during the drought period [46].

2.2. Crop, Soil Moisture and Meteorological Data

In the Netherlands, the *Basisregistratie Gewaspercelen* (BRP), containing parcel-level crop information, is publicly available via the *Publieke Dienstverlening Op de Kaart* (PDOK) [47] web server and is updated annually. The BRP database contains the boundary geometry of agricultural parcels along with the name of the cultivated crop, as well as the geometry and area of the parcel. Major summer crops, namely silage maize, potatoes (for consumption), sugar beets, summer barley and onions are considered in this study. The number of parcels for each crop type in the three study areas is presented in Table 1. For the comparison between the municipalities with and without access to surface water, only maize and potato parcels were considered because the differences in the number of crop parcels between the municipalities are too large to ensure a fair and reliable comparison.

Table 1. Number of crop parcels per study area in 2019.

Crop	Vechtstromen Noord	Scheldestromen	Flevopolder
Silage Maize	4084	1394	300
Sugar Beet	817	2413	660
Potato	541	2722	882
Onion	71	879	767

Annual crop yield information is openly available via Statistics Netherlands (https://opendata.cbs.nl/#/CBS/en/dataset/7100eng/table, accessed on 22 May 2020) [43]. Here, we used the normalized yield (i.e., the total gross yield per harvested hectare, 1000 Kg/Ha) to compare results in the study areas. The normalized gross yield and inter-annual yield differences per province are expressed in 1000 kg/ha for studied crops. Figure 2 shows the normalized gross yield for 2017 per province and inter-annual yield deviation between drought and "normal" years, i.e., 2018–2017 and 2019–2017, respectively. Since the Vechtstromen-Noord study area is located in two provinces, the yield was interpreted by taking the average over Drenthe and Overijssel province data.

VanderSat's daily volumetric surface soil moisture (SM) product (V1.0) is used in this study [48]. The SM products are available at 100 × 100 m resolution on a daily basis from the combined use of Advanced Microwave Scanning Radiometer (AMSR)-2 and Soil Moisture Active Passive (SMAP) microwave satellite sensors retrieved using the Land Parameter Retrieval Model (LPRM) [49–51] . In this study, spatially aggregated volumetric SM data at municipality level were used. The surface soil moisture of the Coevorden, Goes and Zeewolde municipality areas were used for the Vechtstromen-Noord, Scheldestromen and Flevopolder study areas, respectively. Surface soil moisture data from Coevorden, Hardenberg, Tubbergen and Hof van Twente municipalities were used observe the impact of water management decisions. Data discontinuity was observed in the SM products in mid-2019 due to a gap in the SMAP data record.

Meteorological data were acquired from the Royal Netherlands Meteorological Institute (KNMI). KNMI provide daily precipitation data, measured at 48 weather stations throughout the Netherlands. The daily precipitation data acquired by the weather stations in Hoogeveen, Vlissingen and Lelystad were used for the Vechtstromen-Noord, Scheldestromen and Flevopolder study areas, respectively. Data from the Hoogeveen and Twente weather stations were used in the Vechtstromen-Noord area in the analysis related to water management.

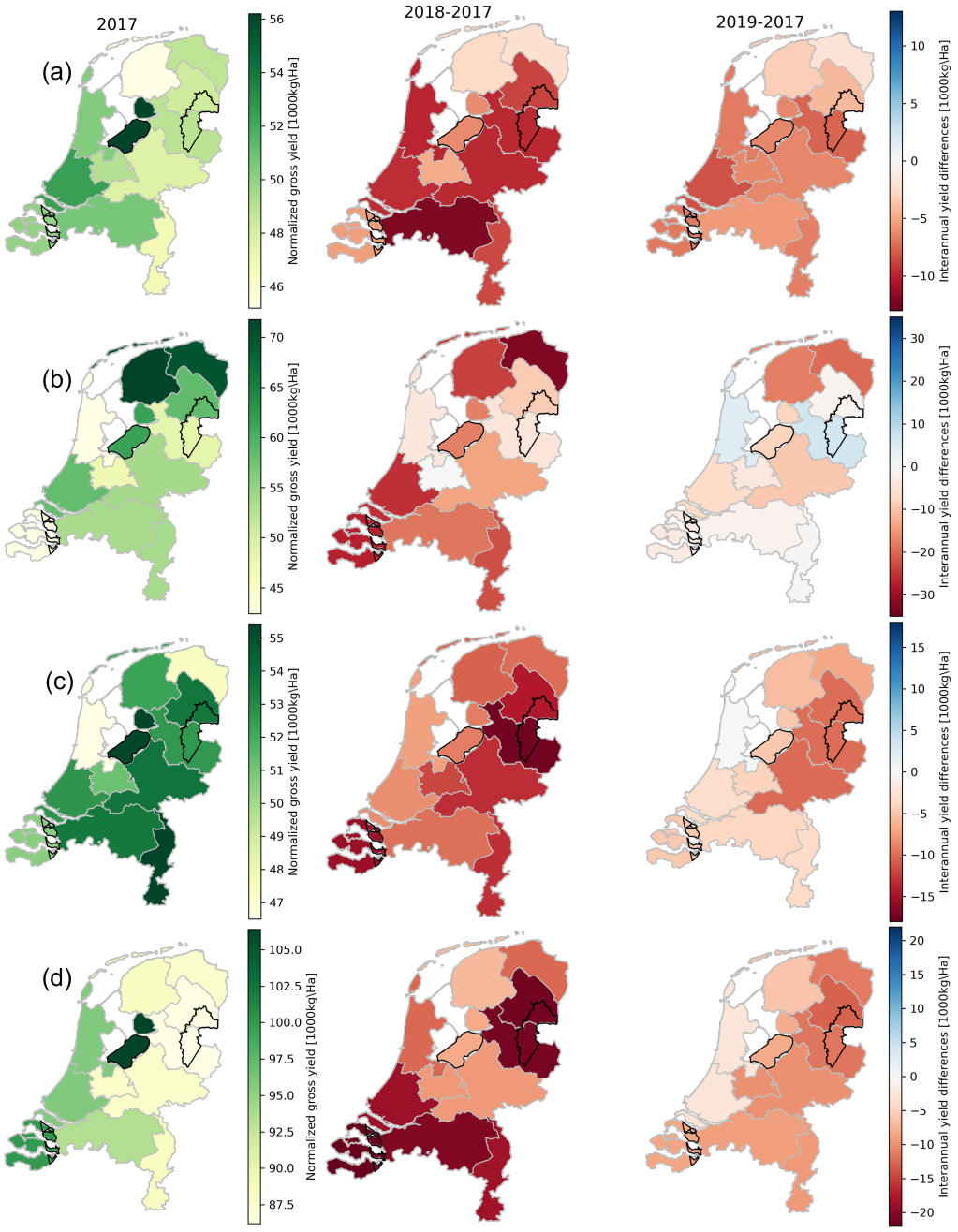

Figure 2. Normalized gross yield and inter-annual yield differences per province expressed in 1000 kg/ha for (**a**) maize, (**b**) onion, (**c**) potato, and (**d**) sugar beet. The left column shows the normalized gross yield for 2017 per province. The middle and right column shows the difference in yield between drought and "normal" years, i.e., 2018–2017 and 2019–2017, respectively. The black polygons indicate the three study areas.

2.3. Sentinel-1 SAR Data

Sentinel-1 SAR GRD data products in interferometric wide (IW) swath mode, available through GEE cloud based services, are used in this study. The Sentinel-1 SAR system consists of two satellites, S1A and S1B, which operate in the C-band (5.45 GHz) with a revisit time of 6 days together. With the combination of different viewing geometries (or relative orbits (RO)) in ascending and descending passes for data acquisition, it is possible to have Sentinel-1 data with a temporal resolution of less than 2 days across Europe. Most of the Netherlands is covered by six different ROs, namely 37, 110, 139, 15, 88 and 161 (Table 2). The swaths of the descending and ascending orbits are shown in Figure 3, respectively.

Table 2. Sentinel-1 orbits characteristic for the study areas.

Relative Orbit	Pass Type	UTC	$\theta_{Vechtstromen-Noord}$	$\theta_{Scheldestromen}$	$\theta_{Flevopolder}$
15	asc	17:16	33.8°–36.3°	-	-
37	des	05:49	34.7°–36.1°	44.4°–45.1°	39.5°–41.6°
88	asc	17:25	42.4°–44.0°	30.1°–31.1°	36.3°–39.5°
110	des	05:58	-	35.7°–41.0°	30.4°–33.7°
139	des	05:41	42.5°–44.4°	-	-
161	asc	17:33	-	36.4°–40.2°	-

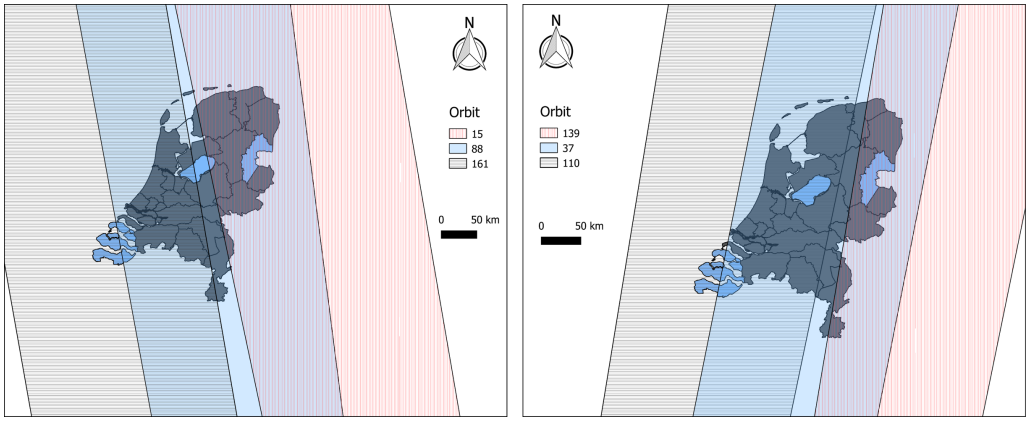

Figure 3. Sentinel-1 descending (**left**) and ascending (**right**) passes and relative orbits covering the Netherlands.

Figure 3 shows that Vechtstromen-Noord is covered by RO 37, 88, 15 and 139. Scheldestromen is covered by RO 161, 110 and parts of 37 and 88. Data acquired from orbit 37 and 88 are used for the analysis of parcels in Scheldestromen since both orbits still cover most of the parcels in that area. Flevopolder is covered by RO 37, 88, 110 and partly covered by RO 15 and 161. Hence, orbits 15 and 161 were not used in the Flevopolder crop parcel analysis. Only data between 1st March and 30th October were considered for each year.

In this study, parcel-level spatially-averaged Sentinel-1 VV and VH backscatter (σ^0) and cross-ratio (VH/VV) values were obtained from the Agricultural SandboxNL database [52,53]. This database was generated from GEE-hosted Sentinel-1 SAR GRD products. GEE-hosted Sentinel-1 data are already corrected for basic SAR pre-processing steps, namely (1) Metadata update with restituted orbit file, (2) Border noise removal after 2018 onward, (3) Thermal noise removal between the sub-swaths, and (4) Radiometric calibration and Terrain correction [28]. The crop parcel-level boundaries in Agricultural SandboxNL were obtained from the annual BRP data [47]. It consists of parcel boundaries, main cultivated crop type information and attributes such as unique OBJECTID and parcel geometry. Parcel-level backscatter values (VV, VH and CR) in the Agricultural SandboxNL database can be queried by crop types, administrative boundaries (province, municipality or user-defined), Sentinel-1 acquisition dates and ROs. Table 3 summarizes the various input datasets, their sources and scales used in this study.

Table 3. Summary of input data used, it's scale and sources.

Data	Data Usage in this Study	Scale	Source(s)
BRP (Crop Parcel Base Register)	To attribute parcel-level crop type information and extract Sentinel-1 backscatter values	Parcel-level	PDOK [47]
Crop yield	To support intra-annual drought observation in time series of Sentinel-1 data	Aggregated at province scale	CBS [43]
Soil type	Information on soil types of the study areas	1:50,000	Steur, 1966 [54]; Hartemink et al., 2013 [55]
Soil moisture	To infer inter-annual variation surface soil moisture over the study areas	Aggregated at municipality scale	VanderSat (Planet) [48]
Precipitation	To infer inter-annual cumulative precipitation over the study areas	Weather stations within the vicinity of study areas	KNMI [56]
Sentinel-1 SAR	To understand drought impact on VH, VV and VH/VV (CR) SAR backscatter data over the study areas	Extracted at parcel level further aggregated over the no. of crop parcels in study areas	Agricultural SandboxNL [52]

2.4. Analysis

Sentinel-1 data for the "normal" year of 2017 were compared to the drought years of 2018 and 2019 to characterize the drought impacts on SAR signals. The VV, VH and CR values were averaged at parcel-level and aggregated per crop type over the studied regions in different relative orbits of the Sentinel-1. The inter-annual comparisons were made by observing the differences in VV, VH backscatter and CR values for 2018 and 2019 compared to 2017. The differences in resulting observations were supported by soil moisture, precipitation, yield, and any openly available ground information during the drought. This comparison will be presented for the Vechtstromen-Noord area because the highest drought impact in 2018 was reported in the north eastern part of the Netherlands [57]. Spatially averaged parcel-level VV, VH and CR values for maize and onion will be presented and discussed. Similar results for potato and sugar beet are provided in supplementary materials. The influence of viewing geometry is considered by comparing data from four relative orbits allowing for differences in incidence angle and between ascending/descending passes.

Figure 2 showed that there were spatial variations in the impact of the droughts on crop yield. This is due to differences in hydrometeorological conditions, soil types and water management decisions during the drought periods. Data from the three study areas were compared to determine if these regional variations in yield correspond to discernible regional differences in the VV, VH and CR values of Sentinel-1 data during the season. Results are presented for maize and onion (potato and sugar beet are in supplementary materials). To ensure that the results are not influenced by differences in viewing geometry, the relative orbits were chosen to minimize the difference in incidence angle.

Finally, data from four municipalities were compared to investigate whether the impact of water use restrictions on the crop development are discernible in the Sentinel-1 data. The spatially-averaged parcel level VV, VH and CR values aggregated per crop type from Coevorden and Hardenberg were contrasted with those in the Tubbergen and Hof van Twente municipalities. Recall that the the first two only have access to groundwater during the droughts, while the last two also have access to surface water. Results will be presented for maize and potato parcels because the number of parcels are comparable.

3. Results

3.1. Influence of Drought on the Seasonal Cycle of Sentinel-1 SAR Data over Agricultural Crops

Spatially-averaged, parcel-level Sentinel-1 data during the 2018 and 2019 drought years were compared to data in a "normal" year (2017).

3.1.1. Maize

Figure 4 shows the time series of Sentinel-1 VV, VH backscatter and cross-ratio (CR, VH/VV) from maize parcels in Vechtstromen-Noord. Maize is typically planted between mid-April and the first week of May, with emergence occuring in mid-May. Silage maize usually ripens in the field and is harvested between mid-September and mid-October [29,58]. Before crop emergence, soil surface roughness and moisture dominate the backscatter response in VV and VH polarizations. Backscatter variations during this period are caused by the rainfall events apparent in the bottom two rows. After emergence, VV and VH backscatter increase rapidly due to soil-vegetation interaction and volume scattering as the crop grows.

Figure 4m shows that the soil moisture in 2018 (~0.07 m^3/m^3) was much lower than that in 2017 (~0.20 m^3/m^3) between day 175 and day 220. During this period, the VV and VH backscatter values in 2018 are ~2 dB lower than the values of 2017. Precipitation around day 220 draws the backscatter values closer to those observed in 2017. Note, however, that the 2018 values decrease more rapidly from DOY 250. The backscatter, but particularly the CR, suggest that the growing season of 2018 was ~30 days shorter than that of 2017. This can be explained by the earlier ripening and harvesting of maize due the dry conditions [59]. The shorter 2018 season also led to a significant drop in yield of 9.1 % compared to 2017 (Figure 2a).

Low soil moisture occurred during the tasseling and flowering phase, which is the most drought sensitive stage according to Kurt Thelen [60]. This is due to a lack of synchronization between silking and shedding of the pollen during pollination. The pollen grains may not remain viable and silking might be delayed. If maize crops have tasselled and shed their pollen while blisters have not appeared yet, the crop will be barren [60].

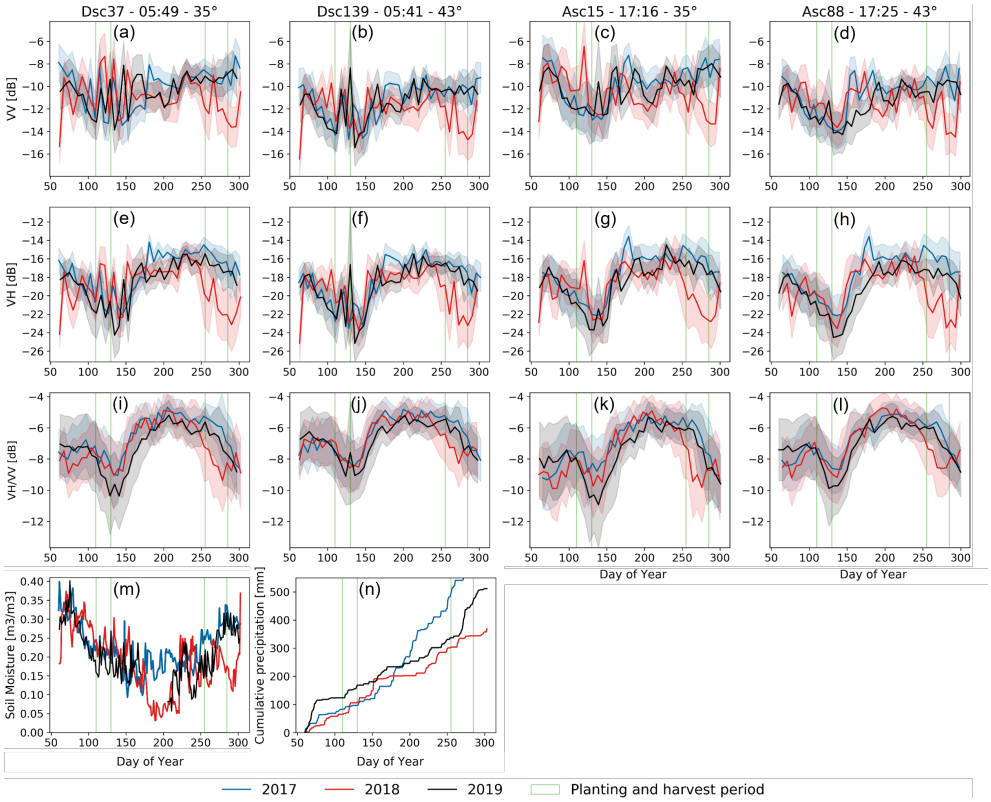

Figure 4. Sentinel-1 descending (RO: 37 and 139) and ascending (RO: 15 and 88) backscatter profiles of VV (**a–d**), VH (**e–h**) and VH/VV (**i–l**) for maize parcels in Vechtstromen-Noord for the years 2017, 2018 and 2019. The title of the columns states whether the data are from a descending (Dsc) or ascending (Asc) overpass, the RO number, the overpass time in UTC and centre incidence angle to the study area. The shaded areas indicate the standard deviation calculated across all parcels. Spatially averaged soil moisture data (**m**) from the Coevorden municipality and cumulative precipitation (**n**) from Hoogeveen weather station. Vertical green lines indicate crop sowing and harvesting periods.

CR values in DOY 130–180 are 1 dB lower in 2019 than in 2017 and 2018. This is likely because the groundwater table and the root zone soil moisture in 2019 had not recovered yet from the drought in 2018, especially in the eastern part of the Netherlands [57].

Furthermore, no large cumulative precipitation increases are observed from DOY 70–105. Thus, it can be assumed that the maize crops were planted and germinated in relatively dry soil. Water stress during the vegetative phase typically reduces leaf and plant size Anami et al. [61]. This would explain the lower VH backscatter and CR values compared to other years. Furthermore, the CR ratio was lower than in 2017 throughout the season. The lower normalized yield (5.9%) for 2019 compared to 2017 infers the lower CR values during the maize growth cycle. The yield reduction is due to anomalies at key moments. The resultant changes to the timing and length of growing season should be considered along with backscatter values to find potential indicators of reduced yield.

Comparing the columns of Figure 4, it is clear that the features discussed above are discernible in all four ROs. The effect of incidence angle is visible in VV and VH backscatter at the crop emergence. The difference in VV backscatter is larger than in VH backscatter, resulting in in a high CR for larger incidence angles.

3.1.2. Onion

Onion is a bulb vegetable typically planted at the end of March and harvested in September [62]. The period between planting and emergence is relatively long for onions. Soil surface roughness and moisture conditions dominate the backscatter contribution during this period. Figure 5 shows that VH backscatter and CR values increase during the leaf development phase (after DOY 140). Similar observations were reported in previous studies [63,64]. VH backscatter and CR decrease as the leaves bend and dry out during the ripening phase of onions. However, VV backscatter keeps increasing due to the increased sensitivity to soil moisture.

The inter-annual differences in the SAR observables were negligible before the onset of drought stress in 2018. The drought period coincides with the stem elongation and bulb development phases of onions. In 2018, all SAR observables started to decrease around DOY 210. CR values in Figure 5i–l show that the 2018 onion growing season was ~10 days shorter than the 2017 season. This is likely because the onions ripened faster and entered senescence earlier. Onions that experience drought stress from the start of the bulb formation stage have a reduced final bulb weight [65] and thus lower crop yield. This decrease is seen in the normalized gross yield data, shown in Figure 2b. The 2018 onion yield is 6.8% lower than the 2017 yield.

Figure 5i–l shows that the 2019 CR values are ~1 dB lower during the emergence and leaf compared to other years. Combined with limited precipitation for a short period in the early season, this led to onion crops being planted into a relatively dry soil and thus a decreased above ground biomass overall compared to other years. The 2019 CR values become similar to the 2017 CR values during ripening and harvest. When comparing the onion yield of 2019 with 2017, the yield was slightly (2.75%) increased (Figure 2b. Hence, the lower CR values before ripening did not translate into a lower yield for onion crops in 2019.

The influence of the satellite overpass time can also be found in the Sentinel-1 backscatter from onion parcels in Figure 5. After VV and especially VH backscatter become relatively stable around DOY 160, VV and VH backscatter rapidly increase in the ascending orbits (Figure 5c,d) around DOY 200. The descending orbits (Figure 5a,b) showed no change around DOY 200 in 2017. In 2018, a small increase was observed only in descending orbit 37. A small increase in VV and VH backscatter is observed around DOY 200 in 2019. However, the rapid backscatter increases observed around DOY 200 in the ascending orbits are not observed in the CR. This suggests that the observations are possibly caused by soil moisture and soil-vegetation interaction.

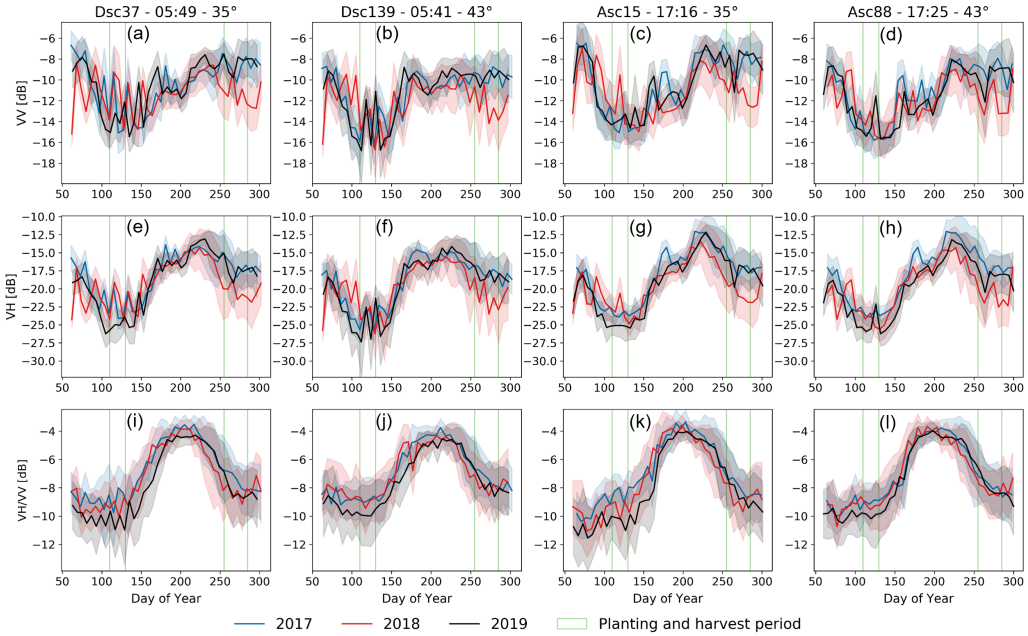

Figure 5. Sentinel-1 descending (RO: 37 and 139) and ascending (RO: 15 and 88) backscatter of VV (**a**–**d**), VH (**e**–**h**) and VH/VV (**i**–**l**) for onion parcels in Vechtstromen-Noord for the years 2017, 2018 and 2019. The title of the columns states whether the data are from a descending (Dsc) or ascending (Asc) overpass, the RO number, the overpass time in UTC and centre incidence angle to the study area. The shaded areas indicate the standard deviation calculated across all parcels. Vertical green lines indicate crop sowing and harvesting periods.

3.2. Regional Variability in the Drought Response Observed Using Sentinel-1

3.2.1. Maize

Figure 6 shows the Sentinel-1 backscatter from maize parcels in the three different study areas. The VH backscatter and CR for 2018 drops rapidly after the DOY 220 in Vechtstromen-Noord and Scheldestromen compared to the Flevopolder region. When focusing on the CR differences after stabilization, it is noticeable that the 2019 values in Vechtstromen-Noord (Figure 6g) are extremely low compared to the 2017 and 2018 values. In Scheldestromen (Figure 6h), and to a lesser extent in Flevopolder (Figure 6i), the 2019 CR is mostly similar to 2018. A likely cause is the soil type in Vechtstromen-Noord, which is dominated by sand. In Scheldestromen and Flevopolder, the soil has a higher clay content.

Furthermore, it can be observed that lack of precipitation events from DOY 70 to 110 leads to the largest drop in surface soil moisture in Vechtstromen-Noord. Surface soil moisture levels during planting were lower in Vechtstromen-Noord than in other study areas. Early dry periods for maize crops can lead to an increase in largest root diameter and a decrease in leaf elongation [2]. This results in a decrease in VH and thus CR values. In addition, the cumulative precipitation shows a dry period in the mid-season for Vechtstromen-Noord. This period is shorter for Scheldestromen and non-existent for Flevopolder, which could explain the decreased CR values in 2019. Another distinct difference between the study areas is the rapid CR decrease due to harvest at the end of the cropping season. Compared to 2017, the CR in 2018 starts decreasing approximately 40, 25, and 10 days earlier in Vechtstromen-Noord, Scheldestromen and Flevopolder, respectively. This is consistent with the normalized gross yield that reduced by 9.1%, 5.4% and 6% compared to the 2017 values (Figure 2a).

For 2019, the CR decreases rapidly approximately 15 and 10 days earlier than in 2017 in Vechtstromen-Noord and Scheldestromen, respectively. In Flevopolder, no early decline is observed for the 2019 CR. The influence of incidence angle on CR values during emergence, can also be observed here, especially in 2019. During emergence, Vechtstromen-Noord has the highest CR values in all years followed by Flevopolder. Scheldestromen shows the low-

est values during emergence. This follows the the incidence angles which are approximately 43°, 38° and 41° for Vechtstromen-Noord, Scheldestromen and Flevopolder, respectively.

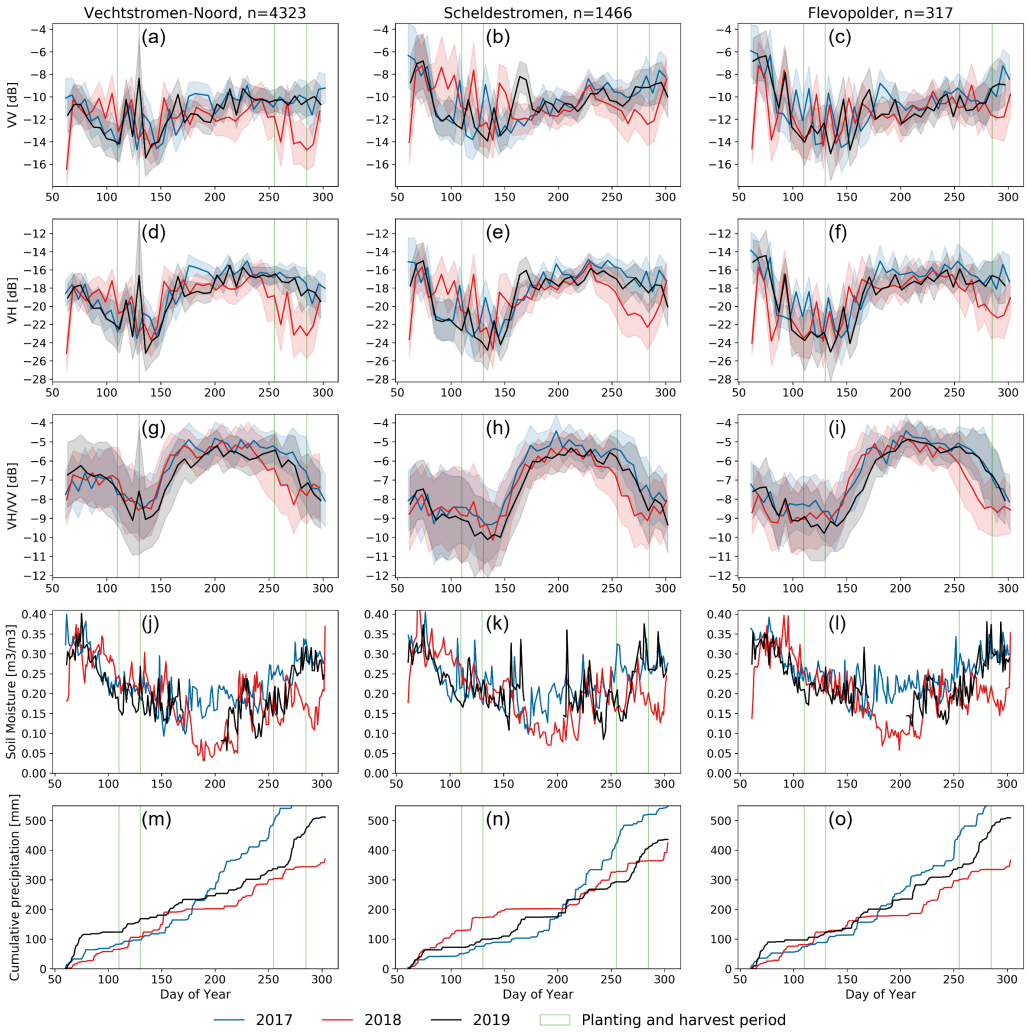

Figure 6. Averaged backscatter profiles of VV (**a**–**c**), VH (**d**–**f**) and VH/VV (**g**–**i**) for maize parcels in Vechtstromen-Noord (left), Scheldestromen (middle) and Flevopolder (right) for the years 2017, 2018 and 2019. The title of the columns states the number of maize parcels in each area. The shaded areas indicate the standard deviation calculated across all parcels. Spatially averaged soil moisture (**j**–**l**) from Coevorden, Goes and Zeewolde municipalities and cumulative precipitation (**m**–**o**) from Hoogeveen, Vlissingen and Lelystad weather stations, respectively, for each area. Vertical green lines indicate crop sowing and harvesting periods.

3.2.2. Onion

Figure 7 shows the Sentinel-1 backscatter from onion parcels in the three different study areas. Onion is a bulb crop and its yield is directly associated with water intake [66], hence drought impacts and regional variabilities are more pronounced in onion compared to other crops. The effect of the 2018 drought are clearly visible in the VH backscatter and CR values for all the studied regions. The early drop in CR values is indicative of the early maturity of onions in 2018. However, among all the studied regions, onion VH backscatter and CR values are lower in Scheldestromen compared to Vechtstromen-Noord and Flevopolder. CR decreases earlier in 2018 in Scheldestromen compared to other areas. Yield data also suggest that the onion crop was hit hardest during the 2018 drought in Scheldestromen.

The normalized gross yield dropped by 6.81%, 27.1% and 17.66% compared to the 2017 drought in Vechtstromen-Noord, Scheldestromen and the Flevopolder, respectively (Figure 2b). Scheldestromen may have been impacted the heaviest due to the lack of available fresh water for irrigation because of the increased salt intrusion in the drought period [67].

Figure 7h shows that the rate of CR decrease is faster in 2018 compared to other areas, and the harvest period is earlier than in other areas. Furthermore, the 2019 CR data clearly display that the root zone soil moisture in Vechtstromen-Noord had not been restored yet [57]. The values during and after planting until DOY 190 are extremely low compared to 2017 and 2018. This is not observed for Scheldestromen since it is situated below sea level and the soil mostly consists of clay. Therefore, the 2019 CR does not show signs of drought early in the season for most crops. In addition, for 2019, CR values are slightly lower in Scheldestromen, while in Vechtstromen-Noord and Flevopolder they are close to the 2017 CR values. These changes are also evident in cumulative rainfall and surface soil moisture plots. After DOY 220, 2019 rainfall is similar to 2018 rainfall for Scheldestromen, whereas in other two areas these are higher than 2018. There is a reduction in onion yield in these two areas as well. However, the observations show that this does not affect the backscatter.

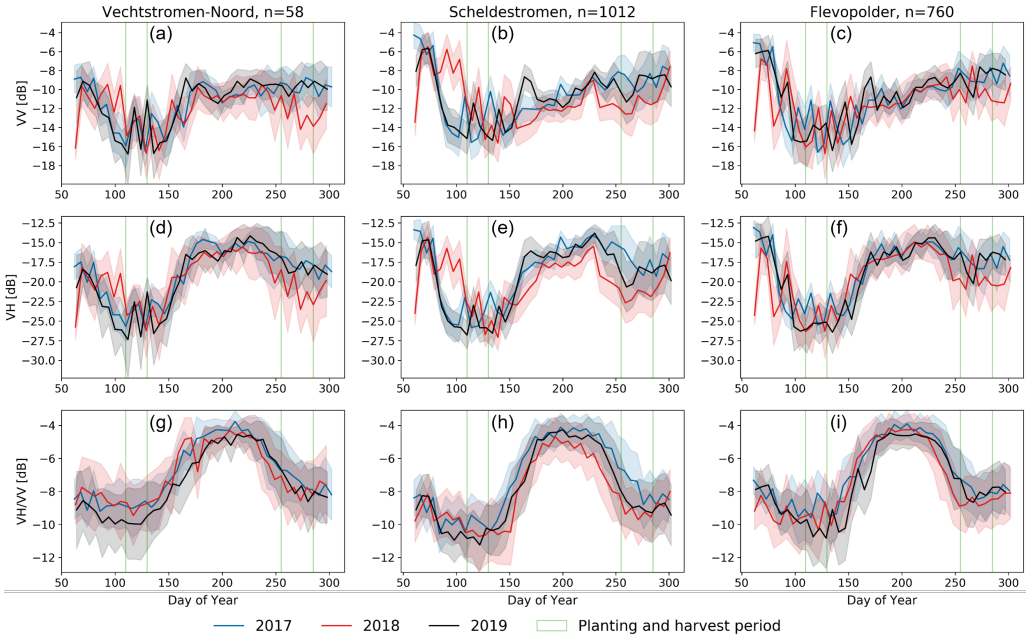

Figure 7. Averaged backscatter profiles of VV (**a**–**c**), VH (**d**–**f**) and VH/VV (**g**–**i**) for onion parcels in Vechtstromen-Noord (left), Scheldestromen (middle) and Flevopolder (right) for the years 2017, 2018 and 2019. The title of the columns states the number of maize parcels in each area. The shaded areas indicate the standard deviation calculated across all parcels. Vertical green lines indicate crop sowing and harvesting periods.

3.3. Observing the Impact of Water Management Decisions

3.3.1. Maize

The 2018 VH/VV ratio of north (Hardenberg and Coevorden) and south (Tubbergen and Hof van Tewnte) municipalities in Vechtstromen starts deviating from 2017 after DOY 230 (Figure 8). It seems that the crop season was shorter for both north and south municipalities and harvesting occurred earlier in 2018. However, the CR in the Tubbergen and Hof van Tewnte municipalities decreases earlier and faster at the end of the season than the CR in the Hardenberg and Coevorden municipalities. A possible explanation is that a higher number of maize parcels in the south municipalities were impacted heavily by the drought due to the ban on open water irrigation, which resulted in an earlier ripening and senescence and thus an early harvest.

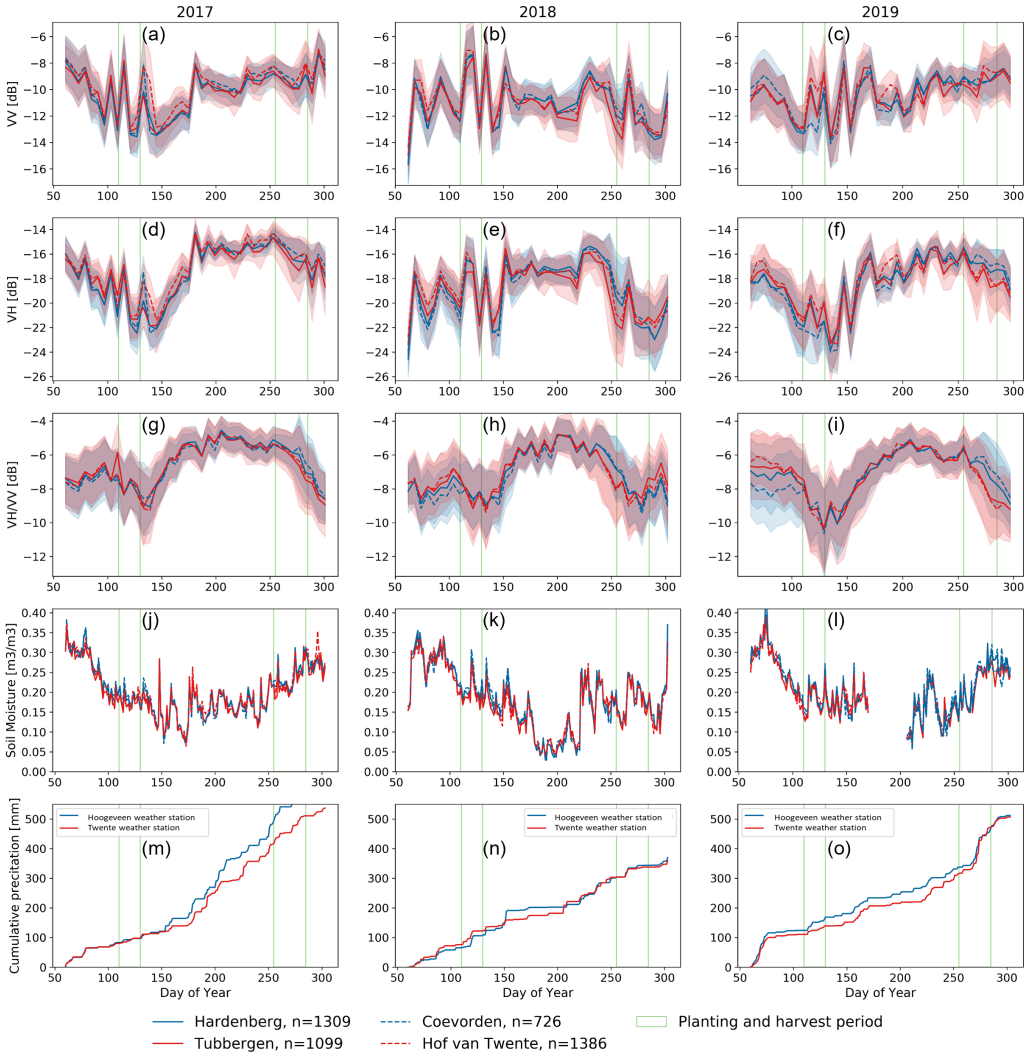

Figure 8. The 2017, 2018 and 2019 time series of Sentinel-1 SAR data (VV (**a**–**c**), VH (**d**–**f**) and VH/VV (**g**–**i**)) from maize parcels in the Coevorden, Hardenberg, Tubbergen and Hof van Twente municipalities. The shaded areas indicate the standard deviation calculated across all parcels. Spatially averaged soil moisture (**j**–**l**) for each municipality and cumulative precipitation (**m**–**o**) from Hoogeveen and Twente weather stations. Vertical green lines indicate crop sowing and harvesting periods.

Furthermore, after DOY 230, the standard deviation of CR in the south municipalities is significantly higher than the north municipalities. This could be because farmers in the south municipalities were only allowed to irrigate from groundwater. Not all farmers are willing to irrigate silage maize with groundwater due to the cost. This may lead to an increase in the backscatter variation across the parcels. In addition, the VH and VV backscatter is significantly lower in the south municipalities during the harvest period around DOY 260.

Coevorden and Hardenberg have very similar CR signatures. The same can be concluded for Tubbergen and Hof van Twente. This can also be seen in Figure 9 where CR values of maize parcels are mapped. The top-left map, which shows the CR ratio on DOY 230, shows regional variability between the north and the south municipalities. This difference increases with each subsequent SAR acquisition shown in Figure 9, i.e., DOY 236, 242 and 248.

In 2019, the differences between the north and south municipalities are negligible until harvest, especially in CR. The CR in the south municipalities starts to decrease around DOY 260, while in the north municipalities, the CR starts to decrease around DOY 275. A high

deviation of CR is also visible in the early growth phase (before DOY 150) of maize in all the municipalities for 2019 compared to other years.

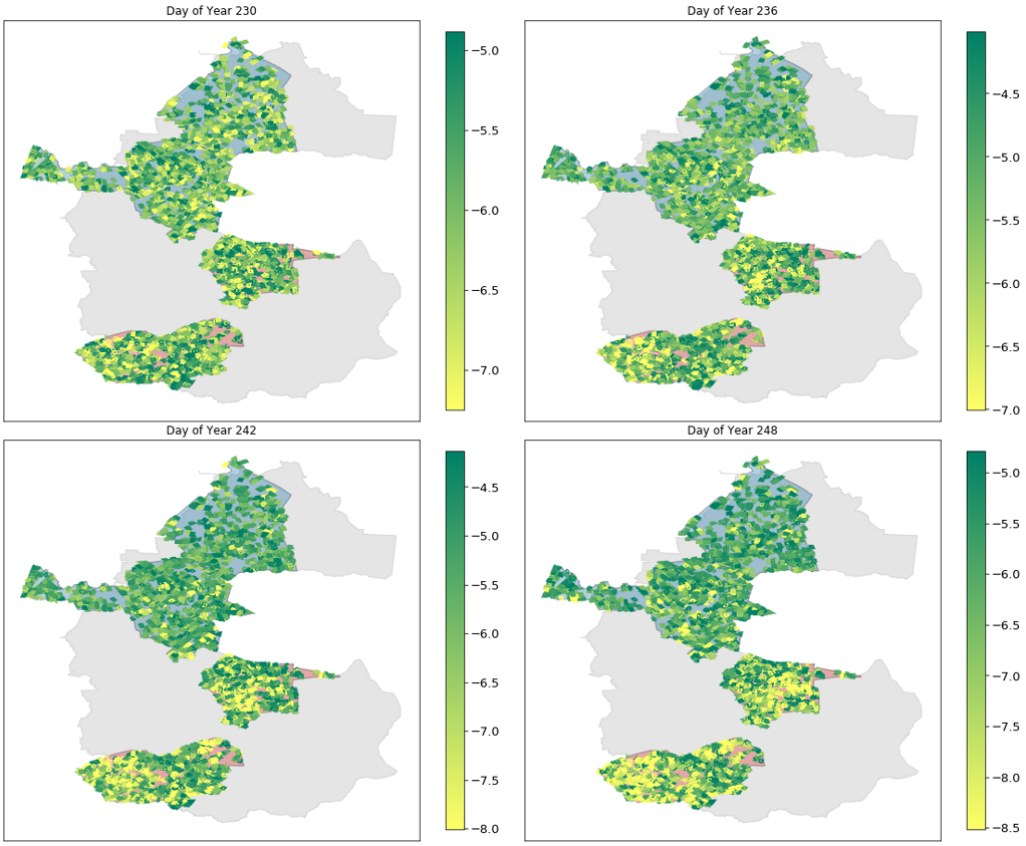

Figure 9. CR values (dB) of maize parcels in the Coevorden, Hardenberg, Tubbergen and Hof van Twente municipalities for the year 2018.

3.3.2. Potato

Potatoes are typically planted between the end of April and the beginning of May, and harvesting starts in September. Potato parcels are easily recognizable due to the deep ridge planting. As a result, the backscatter variation in potato prior emergence is larger due to the deep ridges compared to other crops [68]. Figure 10 shows that in 2017, the backscatter from potato parcels of all the four municipalities is similar. However, the VH backscatter and CR response of potato parcels in 2018 start to diverge around DOY 210 for Tubbergen and Hof van Twente municipalities. Interestingly, CR values are relatively higher for Hof van Twente and lower for Tubbergen than the other two north municipalities (Figure 10h). These differences can be attributed to water management decisions taken in individual areas as cumulative precipitation (Figure 8n) and surface soil moisture (Figure 8k) are comparable among municipalities. The difference in VV, VH and CR values among north and south municipalities is relatively low compared to maize. This is because potato has a higher economic value and is likely to be irrigated with groundwater. Although average CR differences are not high, the standard deviation differences are relatively high between the north and south municipalities. A possible cause is the relatively low number of parcels in Tubbergen, especially in Hof van Twente. The backscatter differences between the north and south municipalities in 2019 are similar but smaller than in 2018.

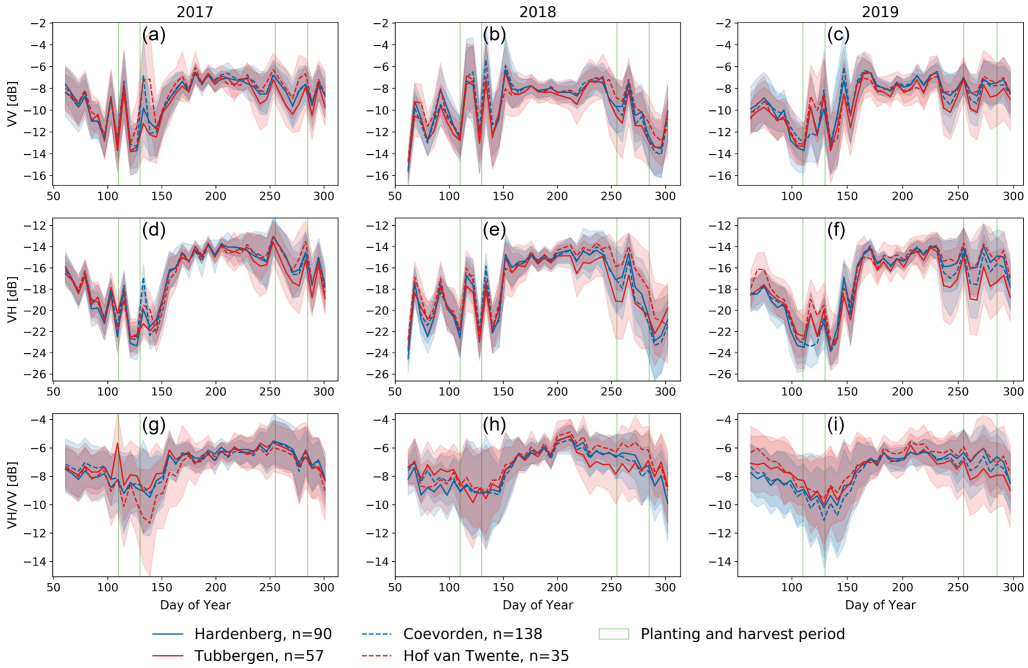

Figure 10. The 2017, 2018 and 2019 time series of Sentinel-1 SAR data (VV (**a**–**c**), VH (**d**–**f**) and VH/VV (**g**–**i**)) from potato parcels in the Coevorden, Hardenberg, Tubbergen and Hof van Twente municipalities. The shaded areas indicate the standard deviation calculated across all parcels. Vertical green lines indicate crop sowing and harvesting periods.

4. Discussion

The interannual variability in the VV, VH backscatter and CR values indicates that SAR signals are sensitive to the drought stress for agricultural crops. However, these changes vary depending on the crop and soil types, water management practices followed in the studied regions. The lower VV and VH backscatter during drought may be caused by dry soil, reduction of VWC and changes in leaf geometry. Furthermore, it was observed that the seasonal cycle of CR for maize and onion was shorter in 2018. However, CR trends for sugar beet and potato did not show a significant difference in 2018 compared to 2017. A possible reason for this is an almost similar drop in VH and VV polarization values in 2018 for sugar beet and potato. Additionally, CR values are relatively lower during the vegetative stages in 2019 compared to 2017 and 2018 for all the crop types.

Regional variability occurs due to many factors, including soil type, hydrometeorological conditions and irrigation policies. Generally, drought responses were most extreme in the Vechtstromen-Noord study area. This is to be expected since this area is most vulnerable to droughts due to its sandy soil. However, onion crops in 2018 were impacted the most in the Scheldestromen area according to yield data (Figure 2). This clearly translated into lower VH backscatter and CR ratio values during and after the drought period.

Among the three SAR observables, CR was found to be a potential candidate to investigate the change of crop growth status due to agricultural drought in 2018 for vertical crops.The utility of CR for identifying key crop growth stages have been discussed in previous studies [31,69,70].

5. Conclusions

To date, there have been few studies focusing on the use of SAR to monitor the effects of drought on crops. Here, we investigated the influence of inter-annual variability in the Sentinel-1 SAR signals over different crops due to the drought in 2018 and 2019 in the Netherlands. The inter-annual variation shows that VH and VV values are lower in the drought period compared to the normal year. The seasonal cycle for CR is found

to be shorter for drought years for both maize and onion. This is caused by faster crop development and thus an earlier harvest due to drier environmental conditions in 2018.

Overall, the influence of the incidence angle on the drought-induced inter-annual variability of Sentinel-1 backscatter time series is found to be limited. On the other hand, the overpass time significantly influences drought-induced inter-annual variability. During drought periods, the drop in VV and VH backscatter was larger in descending orbits (05:45 UTC).

Water management decisions play a crucial role during agricultural drought events. It is observed that for potato crop parcels where open irrigation is allowed, the spatial-temporal variations are similar in all municipalities. Whereas, for maize, a clear difference is observed in CR between the municipalities where irrigation is allowed and those where it is not.

The outcomes of this study revealed the spatial and seasonal variability of SAR signals during the drought years for different crops in the Netherlands where agricultural practices are intensive and regulated. Future research should be extended to understand the responses of different crop types in different agro-climatic regions such as drylands. The sensitivity of the SAR signals also suggests that apart from the backscatter response, other SAR derived observables, interferometric coherence and retrieved bio-geophysical parameters could also be sensitive to the agricultural drought. The use of longer wavelength SAR data may provide a better insight into underlying soil moisture conditions during the drought events. In addition, the synergistic use of optical satellite derived information and SAR observables could combine the sensitivity to spectral characteristics and vegetation water content of the crop canopy affected by the drought.

The research findings demonstrate the Sentinel-1 SAR data contains useful information for water boards, irrigation planners and crop-information services. These data should be included to improve preparedness for future water stress events. They can contribute to decision-making regarding crop parcel water requirements and resource allocation depending on the spatial severity of the drought and economic viability of the crops grown in that area. In the longer-term, monitoring of inter-annual variability in the start and duration of the growing season using SAR data could be included in yield prediction and real-time crop monitoring.

Limitations

- Although Sentinel-1 SAR ensures data availability through the crop growing season, it is not without limitations. Results presented here show the potential value of parcel-level Sentinel-1 backscatter. However, data need to be integrated or synergistically used with high-resolution optical satellite observations to understand within parcel heterogeneity.
- This study also suggests that Sentinel-1 observation geometry (incidence angle and overpass time) influences the backscatter response from different crop types which is relevant for the interpretation of SAR signals. This warrants attention when data from multiple orbits are combined to create a dense time series for near-real monitoring of the crops.
- Previous studies have reported the saturation of C-band SAR signal response to high biomass crops during the peak vegetative stage [71–73]. This could be a potential limitation of using C-band SAR data for seasonal drought observations. However, using a longer wavelength (L-band), SAR data partially overcomes penetration depth limitations. Planned future SAR missions such as NISAR, BIOMASS, ROSE-L will operate at a longer wavelength compared to C-band Sentinel-1 SAR.

Supplementary Materials: The following are available at https://www.mdpi.com/article/10.3390/rs14102435/s1.

Author Contributions: Conceptualization, S.C.S.-D., V.K. and M.S.; methodology, M.S., V.K. and S.C.S.-D.; software, M.S. and V.K.; formal analysis and investigation, M.S., V.K. and S.C.S.-D.; writing—original draft preparation, M.S. and V.K.; writing—review and editing, M.S., V.K. and S.C.S.-D.;

supervision, V.K. and S.C.S.-D.; funding acquisition, S.C.S.-D. All authors have read and agreed to the published version of the manuscript.

Funding: This research is supported by the Dutch network on MIcrowaves for a New Era of Remote sensing of Vegetation for Agricultural monitoring (MINERVA) and Agricultural SandboxNL project. The Netherlands Organisation for Scientific Research (NWO) and Netherlands Space Office (NSO) funded the MINERVA project (NSOKNW.2019.001) and European Space Agency (ESA) funded the Agricultural SandboxNL project (Contract No. 5001025295).

Acknowledgments: This project was partly supported through the MINERVA knowledge network, funded by the Netherlands Space Office (NSO) and the Dutch Research Council (NWO).

Conflicts of Interest: The authors declare no conflict of interest.

References

1. Godfray, H.C.J.; Beddington, J.R.; Crute, I.R.; Haddad, L.; Lawrence, D.; Muir, J.F.; Pretty, J.; Robinson, S.; Thomas, S.M.; Toulmin, C. Food security: The challenge of feeding 9 billion people. *Science* **2010**, *327*, 812–818. [CrossRef] [PubMed]
2. Schmidhalter, U.; Evequoz, M.; Camp, K.H.; Studer, C. Sequence of drought response of maize seedlings in drying soil. *Physiol. Plant.* **1998**, *104*, 159–168. [CrossRef]
3. Wilhite, D.A.; Glantz, M.H. Understanding: The drought phenomenon: The role of definitions. *Water Int.* **1985**, *10*, 111–120. [CrossRef]
4. Li, Y.; Ye, W.; Wang, M.; Yan, X. Climate change and drought: A risk assessment of crop-yield impacts. *Clim. Res.* **2009**, *39*, 31–46. [CrossRef]
5. Hlavinka, P.; Trnka, M.; Semerádová, D.; Dubrovský, M.; Žalud, Z.; Možný, M. Effect of drought on yield variability of key crops in Czech Republic. *Agric. For. Meteorol.* **2009**, *149*, 431–442. [CrossRef]
6. Salehi-Lisar, S.Y.; Bakhshayeshan-Agdam, H. Drought Stress in Plants: Causes, Consequences, and Tolerance. In *Drought Stress Tolerance in Plants, Vol. 1: Physiology and Biochemistry*; Hossain, M.A., Wani, S.H., Bhattacharjee, S., Burritt, D.J., Tran, L.S.P., Eds.; Springer International Publishing: Cham, Switzerland, 2016; pp. 1–16.
7. Lee, J.H.; Kim, C.J. A multimodel assessment of the climate change effect on the drought severity–duration–frequency relationship. *Hydrol. Process.* **2013**, *27*, 2800–2813. [CrossRef]
8. Sheffield, J.; Wood, E.F. Projected changes in drought occurrence under future global warming from multi-model, multi-scenario, IPCC AR4 simulations. *Clim. Dyn.* **2008**, *31*, 79–105. [CrossRef]
9. Hari, V.; Rakovec, O.; Markonis, Y.; Hanel, M.; Kumar, R. Increased future occurrences of the exceptional 2018–2019 Central European drought under global warming. *Sci. Rep.* **2020**, *10*, 1–10. [CrossRef]
10. Spinoni, J.; Vogt, J.V.; Naumann, G.; Barbosa, P.; Dosio, A. Will drought events become more frequent and severe in Europe? *Int. J. Climatol.* **2018**, *38*, 1718–1736. [CrossRef]
11. Palmer, W.C. *Meteorological Drought*; US Department of Commerce, Weather Bureau: Silver Spring, MD, USA, 1965; Volume 30.
12. McKee, T.B.; Doesken, N.J.; Kleist, J. The relationship of drought frequency and duration to time scales. In Proceedings of the 8th Conference on Applied Climatology, Anaheim, CA, USA, 17–22 January 1993; Volume 17, pp. 179–183.
13. Bazrafshan, J.; Hejabi, S.; Rahimi, J. Drought monitoring using the multivariate standardized precipitation index (MSPI). *Water Resour. Manag.* **2014**, *28*, 1045–1060. [CrossRef]
14. Van de Giesen, N.; Hut, R.; Selker, J. The trans-African hydro-meteorological observatory (TAHMO). *Wiley Interdiscip. Rev. Water* **2014**, *1*, 341–348. [CrossRef]
15. Trenberth, K.E.; Dai, A.; Van Der Schrier, G.; Jones, P.D.; Barichivich, J.; Briffa, K.R.; Sheffield, J. Global warming and changes in drought. *Nat. Clim. Chang.* **2014**, *4*, 17–22. [CrossRef]
16. Zhong, R.; Chen, X.; Lai, C.; Wang, Z.; Lian, Y.; Yu, H.; Wu, X. Drought monitoring utility of satellite-based precipitation products across mainland China. *J. Hydrol.* **2019**, *568*, 343–359. [CrossRef]
17. Tucker, C.J.; Choudhury, B.J. Satellite remote sensing of drought conditions. *Remote Sens. Environ.* **1987**, *23*, 243–251. [CrossRef]
18. West, H.; Quinn, N.; Horswell, M. Remote sensing for drought monitoring & impact assessment: Progress, past challenges and future opportunities. *Remote Sens. Environ.* **2019**, *232*, 111291.
19. AghaKouchak, A.; Farahmand, A.; Melton, F.; Teixeira, J.; Anderson, M.; Wardlow, B.D.; Hain, C. Remote sensing of drought: Progress, challenges and opportunities. *Rev. Geophys.* **2015**, *53*, 452–480. [CrossRef]
20. Rhee, J.; Im, J.; Carbone, G.J. Monitoring agricultural drought for arid and humid regions using multi-sensor remote sensing data. *Remote Sens. Environ.* **2010**, *114*, 2875–2887. [CrossRef]
21. Kogan, F. World droughts in the new millennium from AVHRR-based vegetation health indices. *Eos Trans. Am. Geophys. Union* **2002**, *83*, 557–563. [CrossRef]
22. Wieland, M.; Martinis, S. Large-scale surface water change observed by Sentinel-2 during the 2018 drought in Germany. *Int. J. Remote Sens.* **2020**, *41*, 4742–4756. [CrossRef]
23. Zhou, X.; Wang, P.; Tansey, K.; Zhang, S.; Li, H.; Wang, L. Developing a fused vegetation temperature condition index for drought monitoring at field scales using Sentinel-2 and MODIS imagery. *Comput. Electron. Agric.* **2020**, *168*, 105144. [CrossRef]

24. Varghese, D.; Radulović, M.; Stojković, S.; Crnojević, V. Reviewing the Potential of Sentinel-2 in Assessing the Drought. *Remote Sens.* **2021**, *13*, 3355. [CrossRef]
25. McNairn, H.; Shang, J. A review of multitemporal synthetic aperture radar (SAR) for crop monitoring. In *Multitemporal Remote Sensing*; Springer: New York, NY, USA, 2016; pp. 317–340.
26. Steele-Dunne, S.C.; McNairn, H.; Monsivais-Huertero, A.; Judge, J.; Liu, P.; Papathanassiou, K. Radar remote sensing of agricultural canopies: A review. *IEEE J. Sel. Top. Appl. Earth Obs. Remote Sens.* **2017**, *10*, 2249–2273. [CrossRef]
27. Torres, R.; Snoeij, P.; Geudtner, D.; Bibby, D.; Davidson, M.; Attema, E.; Potin, P.; Rommen, B.; Floury, N.; Brown, M.; et al. GMES Sentinel-1 mission. *Remote Sens. Environ.* **2012**, *120*, 9–24. [CrossRef]
28. Google Earth Engine Sentinel-1 Algorithms. Available online: https://developers.google.com/earth-engine/guides/sentinel1?hl=nl (accessed on 20 November 2020).
29. Khabbazan, S.; Vermunt, P.; Steele-Dunne, S.; Ratering Arntz, L.; Marinetti, C.; van der Valk, D.; Iannini, L.; Molijn, R.; Westerdijk, K.; van der Sande, C. Crop monitoring using Sentinel-1 data: A case study from The Netherlands. *Remote Sens.* **2019**, *11*, 1887. [CrossRef]
30. Vreugdenhil, M.; Wagner, W.; Bauer-Marschallinger, B.; Pfeil, I.; Teubner, I.; Rüdiger, C.; Strauss, P. Sensitivity of Sentinel-1 backscatter to vegetation dynamics: An Austrian case study. *Remote Sens.* **2018**, *10*, 1396. [CrossRef]
31. Veloso, A.; Mermoz, S.; Bouvet, A.; Le Toan, T.; Planells, M.; Dejoux, J.F.; Ceschia, E. Understanding the temporal behavior of crops using Sentinel-1 and Sentinel-2-like data for agricultural applications. *Remote Sens. Environ.* **2017**, *199*, 415–426. [CrossRef]
32. Mercier, A.; Betbeder, J.; Baudry, J.; Le Roux, V.; Spicher, F.; Lacoux, J.; Roger, D.; Hubert-Moy, L. Evaluation of Sentinel-1 & 2 time series for predicting wheat and rapeseed phenological stages. *ISPRS J. Photogramm. Remote Sens.* **2020**, *163*, 231–256.
33. Mandal, D.; Kumar, V.; Lopez-Sanchez, J.M.; Bhattacharya, A.; McNairn, H.; Rao, Y. Crop biophysical parameter retrieval from Sentinel-1 SAR data with a multi-target inversion of Water Cloud Model. *Int. J. Remote Sens.* **2020**, *41*, 5503–5524. [CrossRef]
34. Urban, M.; Berger, C.; Mudau, T.E.; Heckel, K.; Truckenbrodt, J.; Onyango Odipo, V.; Smit, I.P.J.; Schmullius, C. Surface Moisture and Vegetation Cover Analysis for Drought Monitoring in the Southern Kruger National Park Using Sentinel-1, Sentinel-2, and Landsat-8. *Remote Sens.* **2018**, *10*, 1482. [CrossRef]
35. Ghazaryan, G.; Dubovyk, O.; Graw, V.; Kussul, N.; Schellberg, J. Local-scale agricultural drought monitoring with satellite-based multi-sensor time-series. *GISci. Remote Sens.* **2020**, *57*, 704–718. [CrossRef]
36. Buras, A.; Rammig, A.; Zang, C.S. Quantifying impacts of the 2018 drought on European ecosystems in comparison to 2003. *Biogeosciences* **2020**, *17*, 1655–1672. [CrossRef]
37. Peters, W.; Bastos, A.; Ciais, P.; Vermeulen, A. A historical, geographical and ecological perspective on the 2018 European summer drought. *Philos. Trans. R. Soc. B* **2020**, *375*, 20190505. [CrossRef] [PubMed]
38. Schuldt, B.; Buras, A.; Arend, M.; Vitasse, Y.; Beierkuhnlein, C.; Damm, A.; Gharun, M.; Grams, T.E.; Hauck, M.; Hajek, P.; et al. A first assessment of the impact of the extreme 2018 summer drought on Central European forests. *Basic Appl. Ecol.* **2020**, *45*, 86–103. [CrossRef]
39. Van Hateren, T.C.; Chini, M.; Matgen, P.; Teuling, A.J. Ambiguous Agricultural Drought: Characterising Soil Moisture and Vegetation Droughts in Europe from Earth Observation. *Remote Sens.* **2021**, *13*, 1990. [CrossRef]
40. Philip, S.; Kew, S.F.; van der Wiel, K.; Wanders, N.; van Oldenborgh, G.J. Regional differentiation in climate change induced drought trends in the Netherlands. *Environ. Res. Lett.* **2020**, *15*, 094081. [CrossRef]
41. Buitink, J.; Swank, A.M.; van der Ploeg, M.; Smith, N.E.; Benninga, H.J.F.; van der Bolt, F.; Carranza, C.D.U.; Koren, G.; van der Velde, R.; Teuling, A.J. Anatomy of the 2018 agricultural drought in The Netherlands using in situ soil moisture and satellite vegetation indices. *Hydrol. Earth Syst. Sci. Discuss.* **2020**, *24*, 6021–6031. [CrossRef]
42. Brakkee, E.; van Huijgevoort, M.; Bartholomeus, R.P. Spatiotemporal development of the 2018–2019 groundwater drought in the Netherlands: A data-based approach. *Hydrol. Earth Syst. Sci. Discuss.* **2021**, *2021*, 1–26.
43. CBS. Arable Crops: Production to Region. Available online: https://opendata.cbs.nl/#/CBS/en/dataset/7100eng/table?ts=1599577672463 (accessed on 22 May 2020).
44. De Loor, G.P.; Hoogeboom, P.; Attema, E.W. The dutch ROVE program. *IEEE Trans. Geosci. Remote Sens.* **1982**, *GE-20*, 3–11. [CrossRef]
45. Satalino, G.; Balenzano, A.; Mattia, F.; Davidson, M.W. C-band SAR data for mapping crops dominated by surface or volume scattering. *IEEE Geosci. Remote Sens. Lett.* **2013**, *11*, 384–388. [CrossRef]
46. Gels, H.; van der Toorn, L. Extreme Droogte 2018: 'Vechtstromen Snakt (Nog Steeds) Naar Water'. 2019. Available online: https://www.stowa.nl/sites/default/files/assets/AGENDA/Agenda202018/2018112220NHI20dag/4.20Hans20Gels-Droogte202018-201920Oost.pdf (accessed on 24 October 2020).
47. PDOK. Dataset: Basisregistratie Gewaspercelen (BRP). Available online: https://www.pdok.nl/introductie/-/article/basisregistratie-gewaspercelen-brp- (accessed on 23 January 2020).
48. De Jeu, R.A.M.; De Nijs, A.H.A.; Van Klink, M.H.W. Method and System for Improving the Resolution of Sensor Data. US Patent 10,643,098, 5 May 2020.
49. Van der Schalie, R.; Parinussa, R.; Renzullo, L.J.; Van Dijk, A.; Su, C.H.; de Jeu, R.A. SMOS soil moisture retrievals using the land parameter retrieval model: Evaluation over the Murrumbidgee Catchment, southeast Australia. *Remote Sens. Environ.* **2015**, *163*, 70–79. [CrossRef]

50. Van der Schalie, R.; Kerr, Y.H.; Wigneron, J.P.; Rodríguez-Fernández, N.J.; Al-Yaari, A.; de Jeu, R.A. Global SMOS soil moisture retrievals from the land parameter retrieval model. *Int. J. Appl. Earth Obs. Geoinf.* **2016**, *45*, 125–134.
51. Owe, M.; de Jeu, R.; Holmes, T. Multisensor historical climatology of satellite-derived global land surface moisture. *J. Geophys. Res. Earth Surf.* **2008**, *113*, F01002. [CrossRef]
52. Kumar, V.; Huber, M.; Rommen, B.; Steele-Dunne, S.C. Agricultural Sandbox NL: A national-scale database of parcel-level, processed Sentinel-1 SAR data. *EarthArXiv Preprint* **2021**. [CrossRef]
53. Kumar, V.; Huber, M.; Shorachi, M.; Rommen, B.; Steele-Dunne, S.C. Agricultural SandboxNL: A crop parcel level database using Sentinel-1 SAR and google earth engine. In Proceedings of the 2021 IEEE International Geoscience and Remote Sensing Symposium IGARSS, Brussels, Belgium, 11–16 July 2021; pp. 6284–6287.
54. Steur, G. De Bodemkaart van Nederland, schaal 1:50,000. Enkele aspecten van de legenda-indeling en de nomenclatuur van de kaarteenheden. *Boor Spade XV* **1966**, *15*, 43–59.
55. Hartemink, A.; Sonneveld, M. Soil maps of the Netherlands. *Geoderma* **2013**, *204*, 1–9. [CrossRef]
56. KNMI Maandsommen Neerslag, Normalen, Anomalieën. Available online: https://www.knmi.nl/nederland-nu/klimatologie/geografische-overzichten/archief/maand/rd (accessed on 24 November 2020).
57. VanderSat. Recovery from the 2018 Drought in the Netherlands. 2019. Available online: http://vandersat.com/blog/recovery-from-the-2018-drought-in-the-netherlands/ (accessed on 29 September 2020).
58. Commissie Samenstelling Aanbevelende Rassenlijst—CSAR. De Aanbevelende Rassenlijst Akkerbouw en Veehouderij 2020. Available online: https://rassenlijst.info/ (accessed on 5 January 2021).
59. Wesselink, M.; Kroonen, B.; de Haan, J. *Toekomst van de Maisteelt op Zandgrond: Overzicht van Huidige Situatie en Mogelijke Maatregelen om de Maisteelt te Verduurzamen*; Technical Report; Stichting Wageningen Research, Wageningen Plant Research, Business unit Open Teelten: Wageningen, The Netherlands, 2019.
60. Thelen, K. Assessing Drought Stress Effects on Corn Yield. 2007. Available online: https://www.canr.msu.edu/news/assessing_drought_stress_effects_on_corn_yield (accessed on 9 September 2020).
61. Anami, S.; De Block, M.; Machuka, J.; Van Lijsebettens, M. Molecular Improvement of Tropical Maize for Drought Stress Tolerance in Sub-Saharan Africa. *Crit. Rev. Plant Sci.* **2009**, *28*, 16–35. [CrossRef]
62. Zaaiuien—Akkerbouwbedrijf Mts. Hoogterp. Available online: http://www.mtshoogterp.nl/zaaiuien.php (accessed on 28 October 2020).
63. Moran, M.S.; Alonso, L.; Moreno, J.F.; Cendrero Mateo, M.P.; de la Cruz, D.F.; Montoro, A. A RADARSAT-2 Quad-Polarized Time Series for Monitoring Crop and Soil Conditions in Barrax, Spain. *IEEE Trans. Geosci. Remote Sens.* **2012**, *50*, 1057–1070. [CrossRef]
64. Mascolo, L. Polarimetric SAR for the Monitoring of Agricultural Crops. Ph.D. Thesis, Università degli Studi di Cagliari, Cagliari, Italy, 2015.
65. Lis, B.R.d.; Ponce, I.; Cavagnaro, J.B.; Tizio, R.M. Studies of Water Requirements of Horticultural Crops: II. Influence of Drought at Different Growth Stages of Onion1. *Agron. J.* **1967**, *59*, 573–576. [CrossRef]
66. Gedam, P.A.; Thangasamy, A.; Shirsat, D.V.; Ghosh, S.; Bhagat, K.P.; Sogam, O.A.; Gupta, A.J.; Mahajan, V.; Soumia, P.S.; Salunkhe, V.N.; et al. Screening of Onion (*Allium cepa* L.) Genotypes for Drought Tolerance Using Physiological and Yield Based Indices Through Multivariate Analysis. *Front. Plant Sci.* **2021**, *12*, 122. [CrossRef]
67. Van Hussen, K.; van de Velde, I.; Läkamp, R.; van der Kooij, S. Economische Schade Door Droogte in 2018. 2019. Available online: https://www.rijksoverheid.nl/documenten/rapporten/2019/08/31/economische-schade-door-droogte-in-2018 (accessed on 15 September 2020).
68. Zhao, L.; Yang, J.; Li, P.; Huang, X.; Shi, L.; Zhang, L. Characterization of the coherent scattering induced by ridging patterns in agriculture by the use of polarimetric SAR imagery. *Int. J. Remote Sens.* **2017**, *38*, 3502–3518. [CrossRef]
69. Harfenmeister, K.; Spengler, D.; Weltzien, C. Analyzing temporal and spatial characteristics of crop parameters using Sentinel-1 backscatter data. *Remote Sens.* **2019**, *11*, 1569. [CrossRef]
70. Vreugdenhil, M.; Navacchi, C.; Bauer-Marschallinger, B.; Hahn, S.; Steele-Dunne, S.; Pfeil, I.; Dorigo, W.; Wagner, W. Sentinel-1 Cross Ratio and Vegetation Optical Depth: A Comparison over Europe. *Remote Sens.* **2020**, *12*, 3404. [CrossRef]
71. Ferrazzoli, P.; Paloscia, S.; Pampaloni, P.; Schiavon, G.; Sigismondi, S.; Solimini, D. The potential of multifrequency polarimetric SAR in assessing agricultural and arboreous biomass. *IEEE Trans. Geosci. Remote Sens.* **1997**, *35*, 5–17. [CrossRef]
72. Blaes, X.; Defourny, P.; Wegmuller, U.; Della Vecchia, A.; Guerriero, L.; Ferrazzoli, P. C-band polarimetric indexes for maize monitoring based on a validated radiative transfer model. *IEEE Trans. Geosci. Remote Sens.* **2006**, *44*, 791–800. [CrossRef]
73. Kraatz, S.; Torbick, N.; Jiao, X.; Huang, X.; Robertson, L.; Davidson, A.; McNairn, H.; Cosh, M.; Siqueira, P. Comparison between Dense L-Band and C-Band Synthetic Aperture Radar (SAR) Time Series for Crop Area Mapping over a NISAR Calibration-Validation Site. *Agronomy* **2021**, *11*, 273. [CrossRef]